ASEAN Journal for Science and Engineering in Materials

Journal homepage: https://ejournal.bumipublikasinusantara.id/index.php/ajsem

Graphite Nanosheets Modified with Carboxymethyl Cellulose as Eco-Friendly Corrosion Inhibitor for Low-Carbon Steel in Saline Environments to Support Sustainable Development Goals (SDGs): An Experimental and Bibliometric Study

Mohamed R. Mohssen[1], Sinan S. Hamdi[1,], Rana A. Anaee[1], Hussain H. Al-Kayiem[2]*

[1]University of Technology-Iraq, Baghdad, Iraq.
[2]University of Hilla, Hillah, Babylon, Iraq.
*Correspondence: E-mail: sinan.s.hamdi@uotechnology.edu.iq

ABSTRACT

Eco-friendly polymeric nanofluids were developed by modifying graphite nanosheets with carboxymethyl cellulose (CMC) to inhibit low-carbon steel corrosion in saline environments. This experimental and bibliometric study combined nanofluid preparation, dispersion assessment, electrochemical testing, surface characterization, and literature mapping to connect material performance with SDGs. The nanocomposite formed a stable dispersion, reduced corrosion activity, and produced an adsorbed protective layer. This protection occurred because CMC provided oxygen-rich functional groups for adsorption, while graphite nanosheets strengthened the chloride barrier. The findings support safer corrosion-control strategies that may reduce toxic inhibitor dependence and improve the durability of steel infrastructure in marine and industrial environments.

ARTICLE INFO

Article History:
Submitted/Received 15 Jan 2025
First Revised 29 May 2026
Accepted 07 Jun 2026
First Available online 07 Jun 2026
Publication Date 01 Dec 2026

Keyword:
Bibliometric analysis;
Carboxymethyl cellulose;
Corrosion inhibition;
Graphite nanosheets;
Low-carbon steel;
Sustainable development goals.

1. INTRODUCTION

Low-carbon steel is widely used in pipelines, storage tanks, seawater systems, desalination units, and oilfield equipment because it is inexpensive, mechanically reliable, formable, and easy to fabricate. However, its long-term service life is strongly limited by corrosion, especially in chloride-rich environments where salinity, temperature, and dissolved ions accelerate metal deterioration. This issue is technically important because corrosion reduces structural reliability, increases maintenance demand, and creates operational and environmental risks in industrial systems (Tiu and Advincula, 2015). In oilfield and marine-related operations, seawater and saline water are frequently involved; therefore, protecting steel infrastructure in saline environments is essential for safer and more sustainable engineering practice (Fathima et al., 2015).

Corrosion inhibitors are commonly used to reduce metal dissolution at the metal-electrolyte interface. Conventional inorganic and organic inhibitors, including chromates, molybdates, nitrites, sulfates, and oxide-based inhibitors, may provide corrosion protection, but their application can be restricted by cost, instability, and environmental toxicity under severe service conditions (Umoren and Eduok, 2016). This limitation has increased interest in green corrosion inhibitors that are biodegradable, less hazardous, and compatible with responsible material use. Such development is relevant to the Sustainable Development Goals (SDGs), particularly sustainable industrialization, responsible production, and protection of water-related environments. Therefore, the design of eco-friendly inhibitors is not only a corrosion-control strategy but also a pathway to improve infrastructure durability while reducing chemical risk (Verma et al., 2018). Polymer-based inhibitors are promising because their molecular structures can contain active functional groups capable of adsorbing on metallic surfaces. Natural and synthetic polymers may form protective films that block aggressive ions and water molecules from reaching active corrosion sites. Among natural polymers, carboxymethyl cellulose (CMC) is attractive because it is water-soluble, biodegradable, film-forming, and rich in hydroxyl and carboxyl groups (Akhlaq et al., 2023). These oxygen-containing groups can interact with steel surfaces and support the formation of an adsorbed barrier layer that suppresses corrosion reactions in aqueous media (Solomon et al., 2010). CMC also has useful thickening, binding, emulsifying, dispersing, and film-forming properties, making it suitable for developing polymeric corrosion-inhibition systems (Ren et al., 2016).

Although CMC can inhibit corrosion through adsorption and film formation, polymer films may become less durable under prolonged exposure, high salinity, and elevated temperature. Carbon-based nanomaterials provide an opportunity to reinforce such polymeric films because of their layered structure, high surface area, and barrier properties. Graphite nanosheets (GNs) have a two-dimensional morphology and can increase the tortuosity of diffusion pathways, thereby limiting the penetration of chloride ions and other corrosive species (Salama et al., 2015). Nevertheless, graphite nanosheets can aggregate in ionic aqueous media due to their hydrophobic nature and interparticle attraction. This aggregation may reduce their effective surface coverage and weaken their practical role as corrosion inhibitors.

Combining GNs with CMC can address this limitation because CMC can act as a stabilizing and film-forming polymer, while GNs can enhance the physical barrier effect of the protective layer. Polymer-assisted graphene-based fluids and green nanomaterial systems can improve corrosion resistance in chloride-containing environments, although performance depends on

dispersion quality, concentration, substrate type, and exposure condition (Borode et al., 2021). Environmentally oriented nanofluids can provide effective protection in saline media (Shao et al., 2024). Therefore, CMC-modified GNs are expected to provide a synergistic corrosion-inhibition effect through improved dispersion, surface adsorption, and barrier formation. In addition to experimental evaluation, bibliometric analysis can strengthen the positioning of this research within the broader development of sustainable corrosion inhibitors, green nanomaterials, and SDGs-related materials engineering. Bibliometric mapping helps identify publication trends, dominant research themes, and the relationship between corrosion protection, polymeric inhibitors, nanomaterials, and sustainability. This approach is useful because the current research direction is not only focused on technical inhibition efficiency but also on the transition from toxic inhibitors to safer and more sustainable materials. Thus, combining experimental corrosion testing with bibliometric analysis provides both practical material evidence and a broader research-contextual contribution.

This study aims to develop CMC-modified graphite nanosheets as an eco-friendly polymeric nanofluid for inhibiting corrosion of low-carbon steel in saline environments and to position the work within SDGs-oriented sustainable corrosion research through bibliometric analysis. The experimental method involved two-step nanofluid preparation, ultrasonication, colloidal stability assessment, electrochemical measurements, and surface characterization. The bibliometric component was used to map the research landscape related to green corrosion inhibitors, polymer nanocomposites, and sustainable materials. The novelty of this work lies in integrating CMC-stabilized GNs as a corrosion-inhibition system with bibliometric insight to support SDGs-oriented development of safer protective materials for steel infrastructure.

2. MATERIALS AND METHODS

2.1. Materials

CMC powder was obtained from TM Media Ltd., India, with an approximate molecular weight of 90,000 g/mol. Graphite was purchased from a local commercial supplier in Iraq, and sodium chloride was obtained from Loba Chemie Pvt. Ltd., India. A 3.5 wt.% NaCl solution was used as the saline corrosive medium to simulate chloride-rich environments. Low-carbon steel specimens with dimensions of 1 × 1 × 0.6 cm were used as working samples. The steel composition consisted of 0.129 wt.% C, 0.284 wt.% Mn, 0.119 wt.% Si, 0.02197 wt.% P, 0.0151 wt.% Cr, 0.004 wt.% Mo, 0.0037 wt.% Al, 0.002 wt.% V, and Fe as the balance. Before corrosion testing, the exposed surface area was fixed at 1 × 1 cm, mounted in a holder, polished sequentially using silicon carbide papers of 600, 800, 1000, and 1200 grades, cleaned with absolute ethanol, and dried using an air jet.

2.2. Preparation of CMC-GNs Polymeric Nanofluids

CMC-GNs polymeric nanofluids were prepared using a two-step method, as illustrated in **Figure 1**. First, CMC was dissolved in 100 mL of distilled water at a fixed concentration of 1 g/L under magnetic stirring for 2 h to obtain a homogeneous polymer solution. Then, 3.5 g of NaCl was added to the polymer solution and stirred for 1 h at room temperature to form the saline polymer medium. Graphite nanosheets were introduced at concentrations of 0.1, 0.5, and 1 g/L and stirred for 1 h. The suspension was then ultrasonicated for 2 h in a cold bath to improve nanosheet dispersion and obtain homogeneous CMC-GNs nanofluids.

2.3. Characterization of the Polymeric Nanocomposite

The functional groups and chemical interactions of CMC, graphite nanosheets, CMC-GNs, and the protective film formed on the steel surface were analyzed using Fourier-transform infrared spectroscopy in the range of 4000-400 cm^{-1}. The crystalline and phase structures of graphite nanosheets and CMC-GNs were examined using X-ray diffraction with a scanning range of 10-80°. The morphology, size, and sheet structure of graphite nanosheets and CMC-GNs were observed using transmission electron microscopy and scanning electron microscopy. Energy-dispersive X-ray spectroscopy was used to identify elemental changes on the steel surface after immersion and to support the interpretation of the inhibition mechanism.

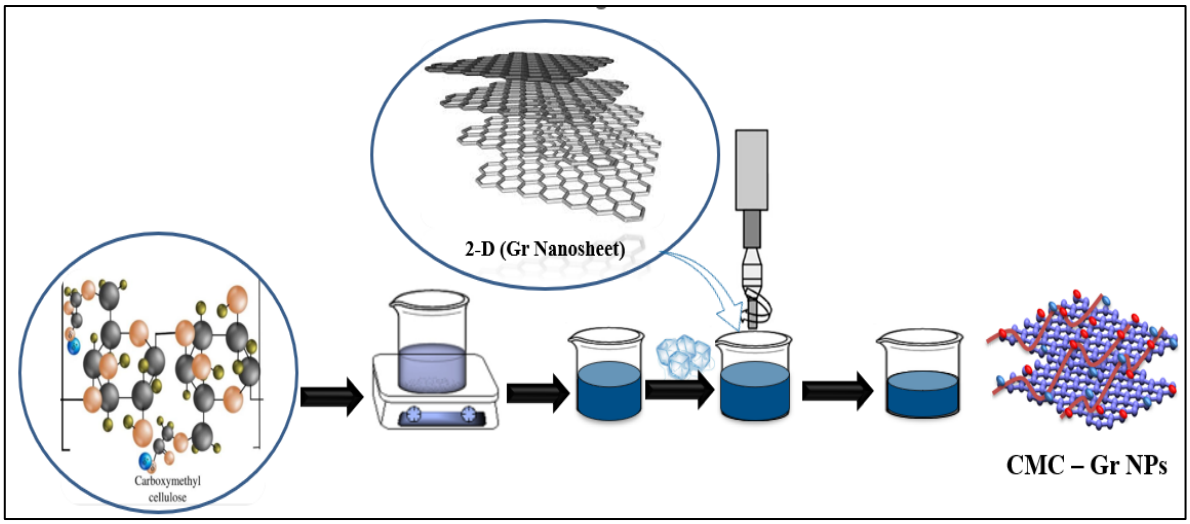

Figure 1. A combination of graphite with CMC via a two-step method.

2.4. Nanofluid Stability Evaluation

The colloidal stability of CMC-GNs nanofluids in 3.5 wt.% NaCl solution was evaluated using zeta potential, hydrodynamic particle size, and UV-Vis spectrophotometry. Zeta potential and particle size measurements were used to determine electrostatic stability and dispersion quality. UV-Vis analysis was conducted over the wavelength range of 190-1100 nm to monitor optical absorbance and long-term dispersion behavior. Stability was examined after aging in saline media and under different temperatures to evaluate whether the polymeric nanofluids could maintain dispersion under conditions relevant to practical saline environments.

2.5. Electrochemical Corrosion Measurements

Electrochemical corrosion measurements were performed using a potentiostat equipped with a three-electrode cell, as shown in Figure 2. A low-carbon steel specimen was used as the working electrode, a saturated calomel electrode was used as the reference electrode, and platinum was used as the counter electrode. The tests were carried out in 3.5 wt.% NaCl solution without and with CMC-GNs nanofluids at different concentrations and temperatures. Open-circuit potential was first recorded until a stable condition was obtained. Potentiodynamic polarization was then performed to determine corrosion potential, corrosion current density, and anodic and cathodic Tafel slopes. Electrochemical impedance spectroscopy was also conducted to evaluate charge-transfer behavior and corrosion resistance.

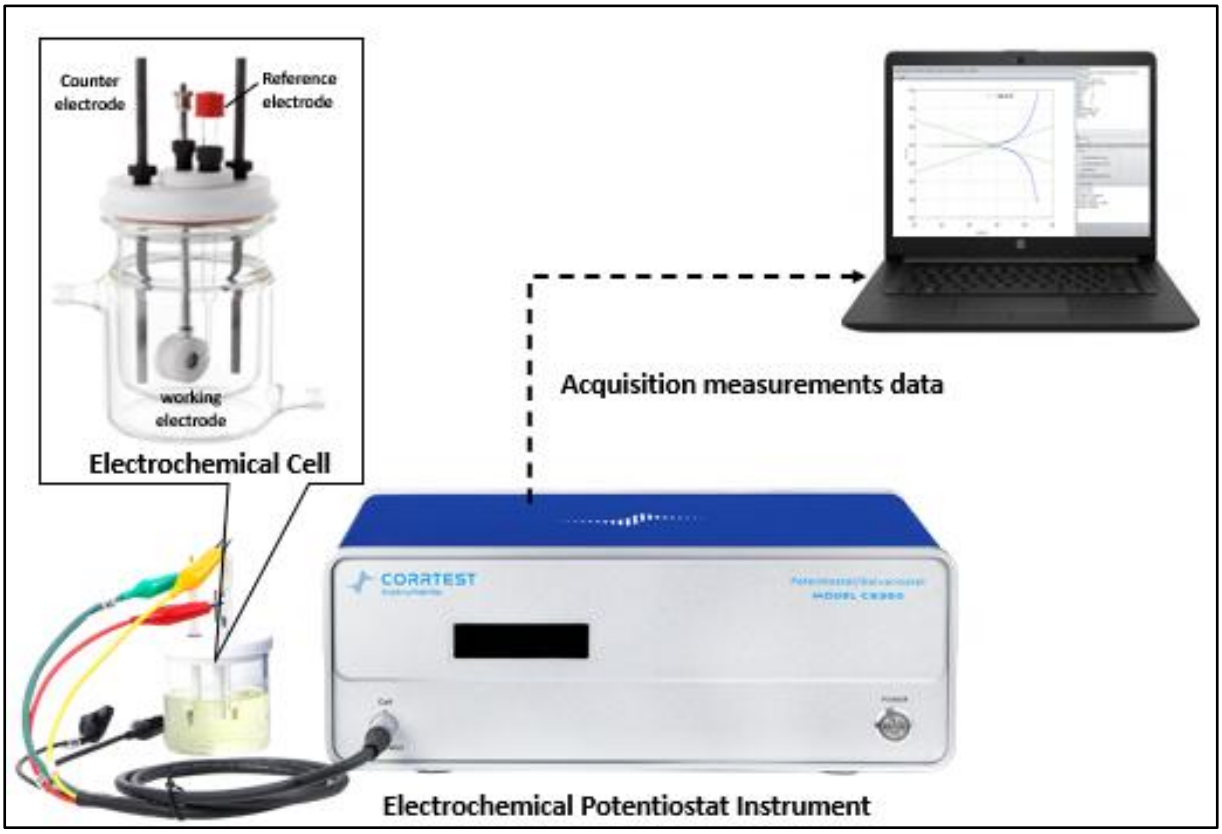

Figure 2. Schematic diagram of the electrochemical potentiostat utilized for OCP and EIS measurements.

The polarization resistance was calculated from the corrosion current density and Tafel slopes using **Equation (1)** (Anaee, 2014).

$$R_p = \frac{b_c \times b_a}{2.303 \times i_{corr}(b_c + b_a)} \quad (1)$$

where R_p is the polarization resistance (Ω.cm²), i_{corr} is the corrosion current density (A/cm²), b_a is the anodic Tafel slope (V/dec), and b_c is the cathodic Tafel slope (V/dec).

The inhibition efficiency was calculated using the corrosion current density values in the absence and presence of CMC-GNs in the saline solution, as shown in **Equation (2)** (Najm et al., 2022a; Najm et al., 2022b).

$$IE = \left[1 - \frac{i_{in\ the\ presence\ of\ CMC-GNs}}{i_{in\ the\ absence\ of\ CMC-GNs}}\right] \times 100 \quad (2)$$

where *IE* is the inhibition efficiency (%), i is the corrosion current, which is in the presence and absence of CMC-GNs.

2.6. Bibliometric Analysis

Bibliometric analysis was conducted to map the publication trend of corrosion inhibitor research and to position the present experimental study within the broader context of sustainable materials development. The bibliographic data were collected from the Scopus database using the search query TITLE-ABS-KEY (corrosion AND inhibitor). The search covered publications from 1928 to 2025 and focused on the number of documents published per year.

The annual publication trend was analyzed to identify the growth pattern of corrosion inhibitor research and its relevance to sustainable corrosion-control strategies. The bibliometric output was used to support the discussion on the contribution of eco-friendly CMC-GNs inhibitors to SDGs-oriented materials research.

3. RESULTS AND DISCUSSION

3.1. Characterization of CMC-GNs Nanocomposite

FTIR analysis was used to identify the functional groups of CMC, graphite nanosheets, and CMC-GNs, as shown in **Figure 3**. The CMC-GNs spectrum combined the characteristic bands of both CMC and graphite, indicating successful interaction between the polymer chains and graphite surface. The broad hydroxyl vibration and carboxyl-related absorption confirmed the presence of oxygen-containing functional groups that are important for adsorption on the steel surface. The graphite-related carbon structure was also retained, suggesting that the modification process did not destroy the main graphitic framework. This interaction is important because hydroxyl and carboxyl groups can support adsorption and protective-film formation on metallic surfaces (Xu and Suslick, 2011).

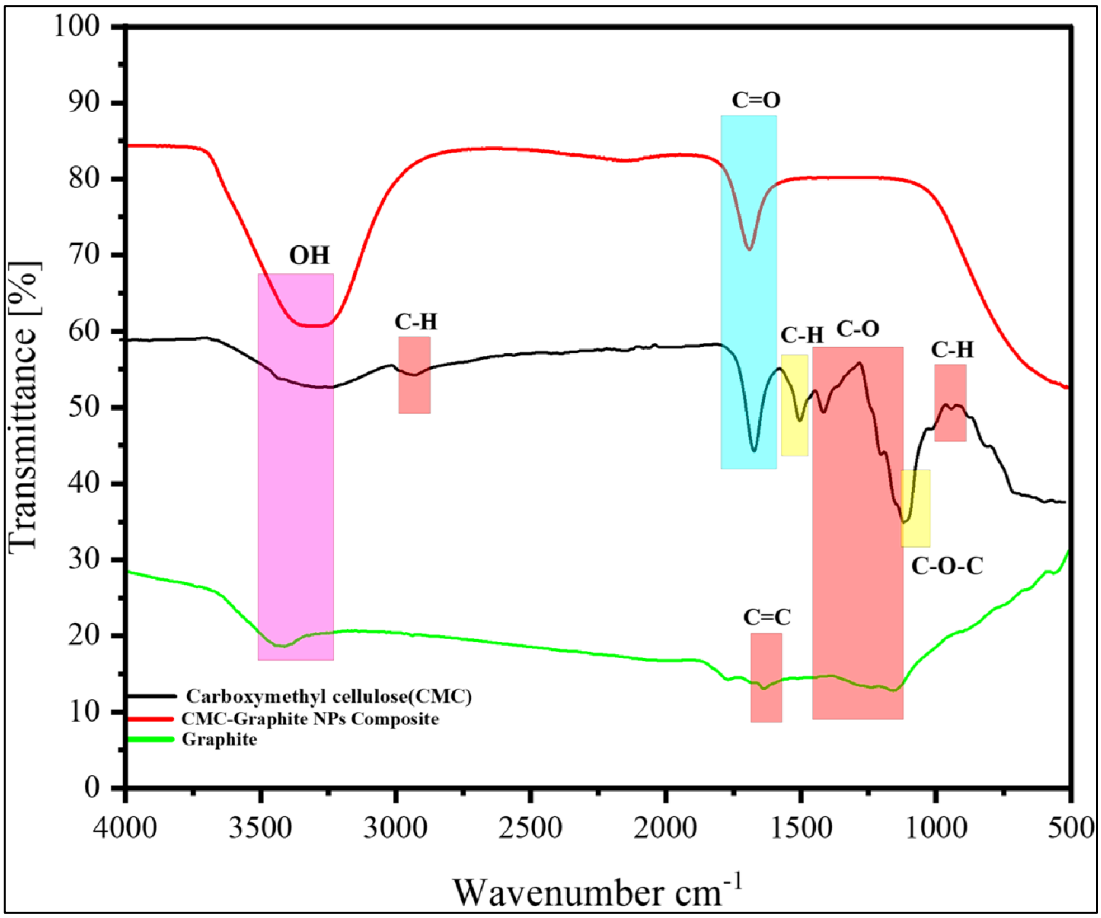

Figure 3. FTIR spectroscopy for graphite, CMC, and CMC-GNs composite.

SEM analysis confirmed the morphological changes of graphite nanosheets after modification with CMC, as shown in **Figure 4**. **Figure 4a** shows the unmodified graphite with compact, stacked, and plate-like multilayer sheets, indicating strong interlayer attraction and limited separation between graphite layers. At higher magnification, **Figure 4b** further reveals that the graphite surface remains relatively intact, with dense sheet aggregation and sharp

edges. After modification with CMC, **Figure 4c** shows a more separated sheet morphology, where graphite layers appear partially exfoliated and more uniformly distributed in the polymer matrix. **Figure 4d** confirms that the CMC-GNs structure contains thinner and less aggregated nanosheets, suggesting that CMC and ultrasonication assisted the dispersion process and reduced graphite restacking. This morphological change indicates that CMC acted as a stabilizing and dispersing polymer, while sonication promoted sheet separation during nanocomposite preparation (Ghanem and Abdel Rehim, 2018).

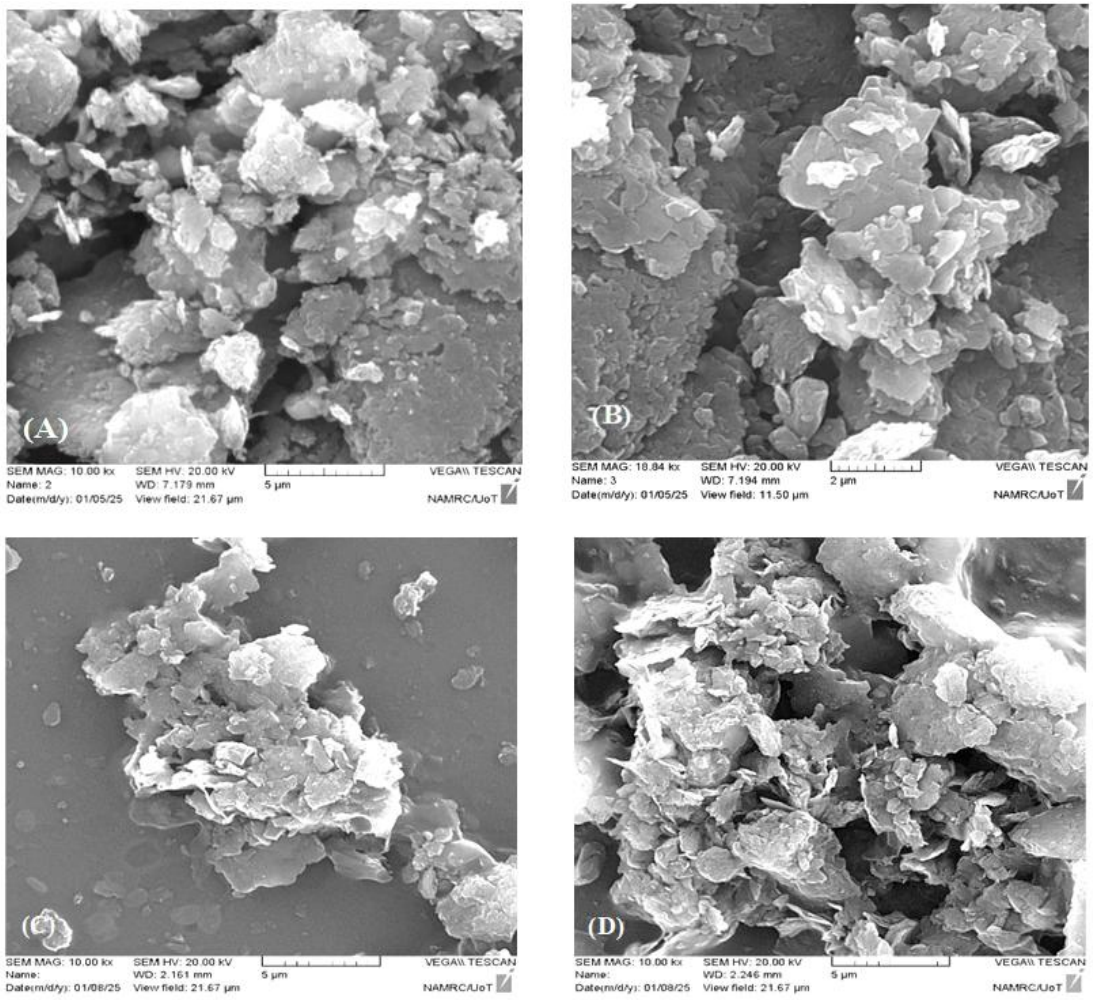

Figure 4. SEM images of graphite and CMC-GNs nanosheets: (a) unmodified graphite showing compact stacked multilayer sheets; (b) unmodified graphite at higher magnification showing dense aggregation and intact sheet edges; (c) CMC-GNs showing more separated and partially exfoliated nanosheets; and (d) CMC-GNs at higher magnification showing thinner, less aggregated, and more uniformly distributed nanosheets.

TEM analysis further confirmed the structural difference between unmodified graphite and CMC-GNs, as shown in **Figure 5**. Figure 5a shows the unmodified graphite nanosheet with a relatively stacked and overlapping sheet structure, indicating strong interlayer interaction and limited exfoliation. In contrast, Figure 5b shows CMC-GNs with thinner, more transparent, and more separated nanosheets. The reduced lateral size and clearer sheet edges indicate that the graphite layers were exfoliated and fragmented during ultrasonication. The presence of CMC also helped stabilize the separated nanosheets by

reducing restacking and improving dispersion in the polymeric medium. This morphology confirms that CMC acted as a dispersing and stabilizing agent during CMC-GNs preparation (Ghanem and Abdel Rehim, 2018).

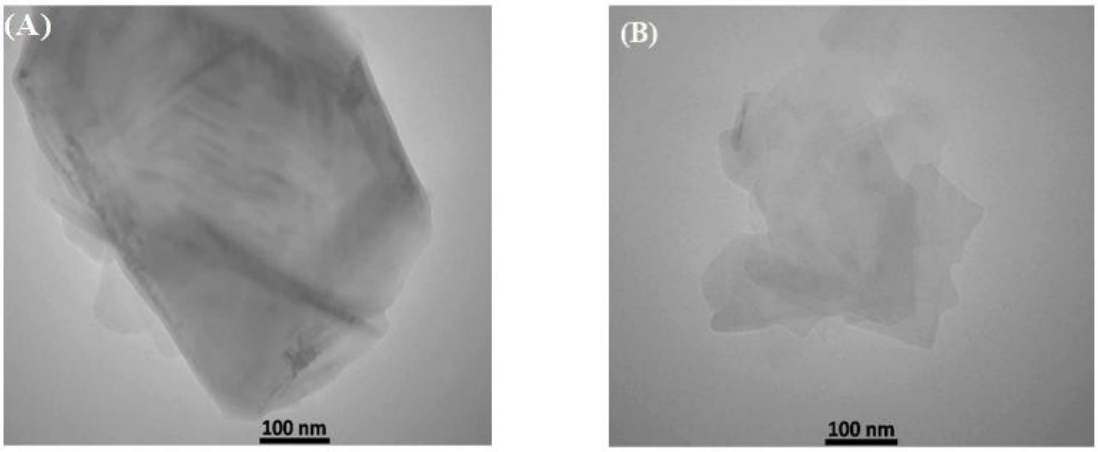

Figure 5. TEM images of graphite-based nanosheets: (a) unmodified graphite nanosheet showing stacked and overlapping sheet morphology; and (b) CMC-GNs showing thinner, more transparent, and more separated nanosheets after CMC-assisted ultrasonication.

The XRD patterns in **Figure 6** further support the successful formation of CMC-GNs. Graphite showed a sharp characteristic diffraction peak related to the ordered graphitic structure, while CMC displayed semi-crystalline polymer features. After modification, CMC-GNs retained the main graphite peak with lower intensity, indicating that the graphite structure was preserved while its crystalline stacking was reduced. This result supports the interpretation that ultrasonication and CMC modification improved nanosheet separation without causing severe structural damage. Similar graphite and CMC diffraction characteristics have been reported for exfoliated graphite and cellulose-based materials (Sharma et al., 2015; Kumar and Priyadarshi, 2020).

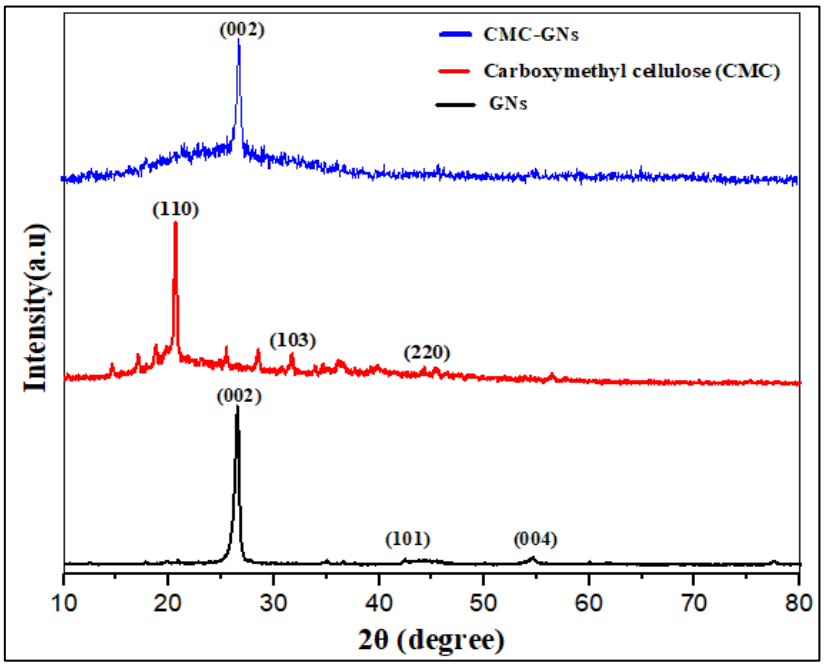

Figure 6. XRD patterns of CMC natural polymer, unmodified graphite nanosheet, and CMC-covered GNs.

3.2. Dispersion Stability of CMC-GNs Nanofluids

The dispersion stability of CMC-GNs nanofluids in saline medium was evaluated using zeta potential and particle size distribution, as shown in **Figure 7**. **Figure 7a** shows that all CMC-GNs nanofluids had negative zeta potential values, indicating that electrostatic repulsion was sufficient to reduce nanosheet aggregation in the saline medium. The lowest GNs concentration showed the highest negative zeta potential, suggesting better colloidal stability because CMC could provide more effective surface coverage and steric stabilization at lower nanosheet loading. In general, colloidal systems with zeta potential values above the common stability threshold show stronger resistance to aggregation, which supports the stable dispersion behavior of the CMC-GNs nanofluids (Yu and Xie, 2012). **Figure 7b** presents the particle size distribution of CMC-GNs nanofluids after dispersion in a saline medium. The hydrodynamic size increased as the GN concentration increased, indicating that higher nanosheet loading promoted partial aggregation or reduced dispersion uniformity. The smallest particle size was obtained at the lowest GNs concentration, confirming that this formulation had the most stable dispersion. These results show that the stability of CMC-GNs nanofluids depends on the balance between nanosheet concentration and CMC coverage. Therefore, the low-concentration CMC-GNs formulation was more suitable for corrosion inhibition because stable dispersion can improve inhibitor distribution and surface adsorption on low-carbon steel.

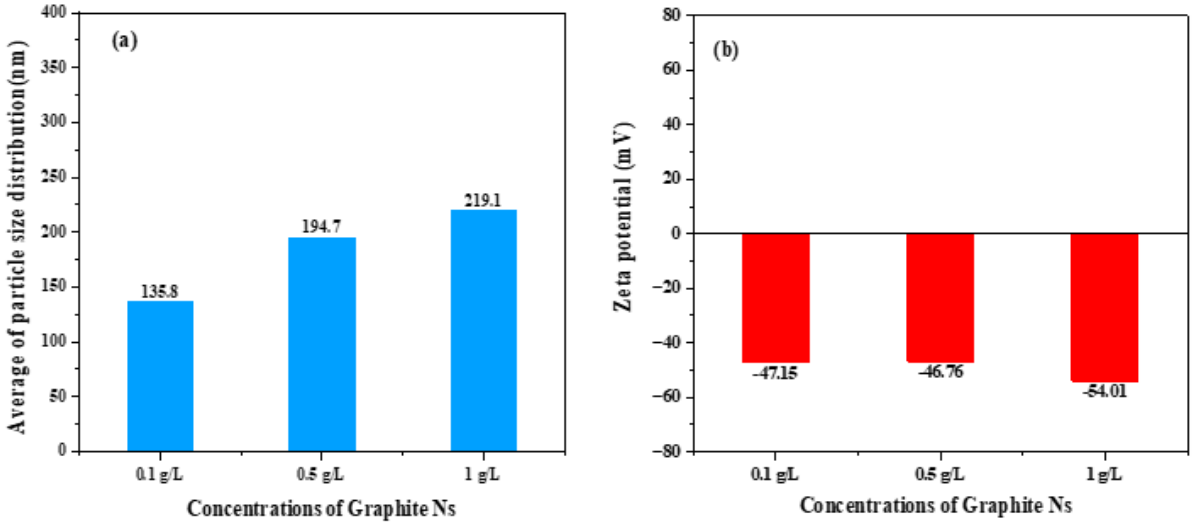

Figure 7. Colloidal stability of CMC-GNs nanofluids in saline medium: (a) zeta potential values showing negative surface charge and electrostatic stability at different GNs concentrations; and (b) particle size distribution showing increased hydrodynamic size with increasing GNs concentration.

UV-Vis spectroscopy was used to evaluate the optical stability of CMC-GNs nanofluids under saline and thermal conditions. **Figure 8** shows that the characteristic absorbance of graphite-based dispersion was maintained at different temperatures, especially at low CMC-GNs concentration. **Figure 9** further confirms that the absorbance remained relatively stable after aging, indicating that CMC-GNs could resist sedimentation and aggregation in high-salinity media. This result is relevant for corrosion protection because a stable inhibitor dispersion is necessary to ensure continuous transport and adsorption of active materials on the steel surface during exposure.

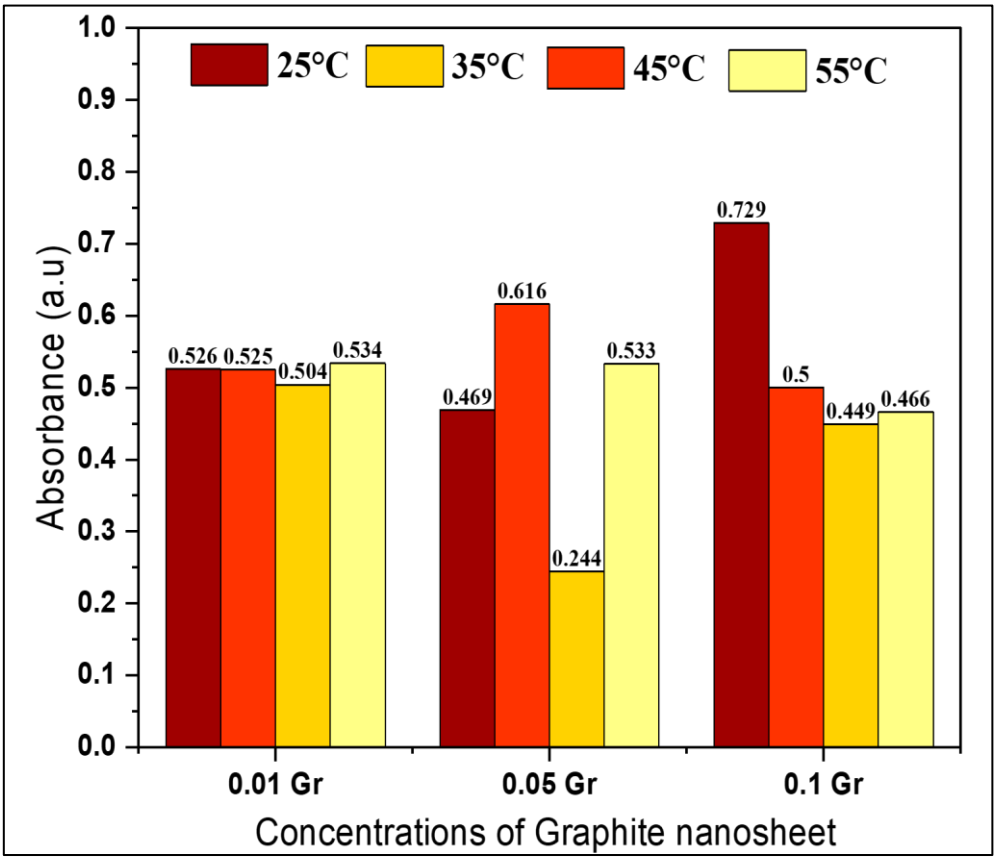

Figure 8. Variation in optical absorbance of CMC-GNs with different concentrations in high saline media and different temperatures.

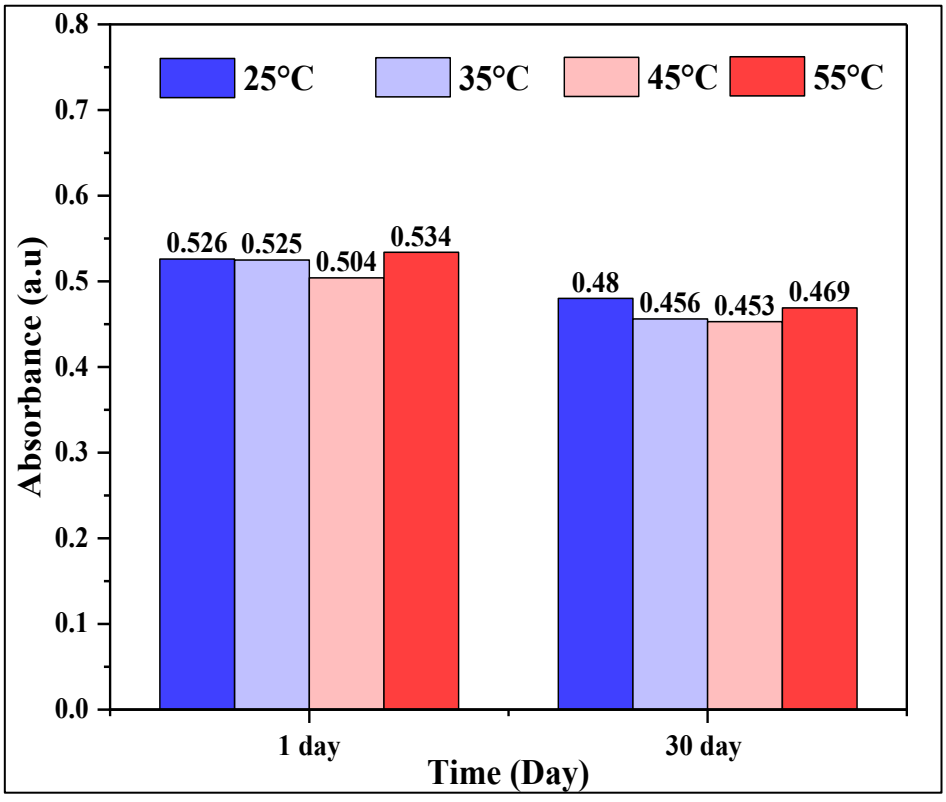

Figure 9. Dispersion stability of CMC-GNs nanofluids in high saline media at different temperatures versus ageing time.

3.3. Electrochemical Corrosion Behavior

Open-circuit potential measurements showed that the addition of CMC and CMC-GNs shifted the potential of low-carbon steel in saline media, as shown in **Figure 10**. This shift indicates that the inhibitor affected the electrochemical reactions occurring on the steel surface. The presence of CMC-GNs promoted the formation of a protective layer, which reduced the direct contact between steel and chloride-containing electrolyte. The potential shift also suggests that the inhibitor influenced both anodic metal dissolution and cathodic reactions, supporting its mixed-type inhibition behavior.

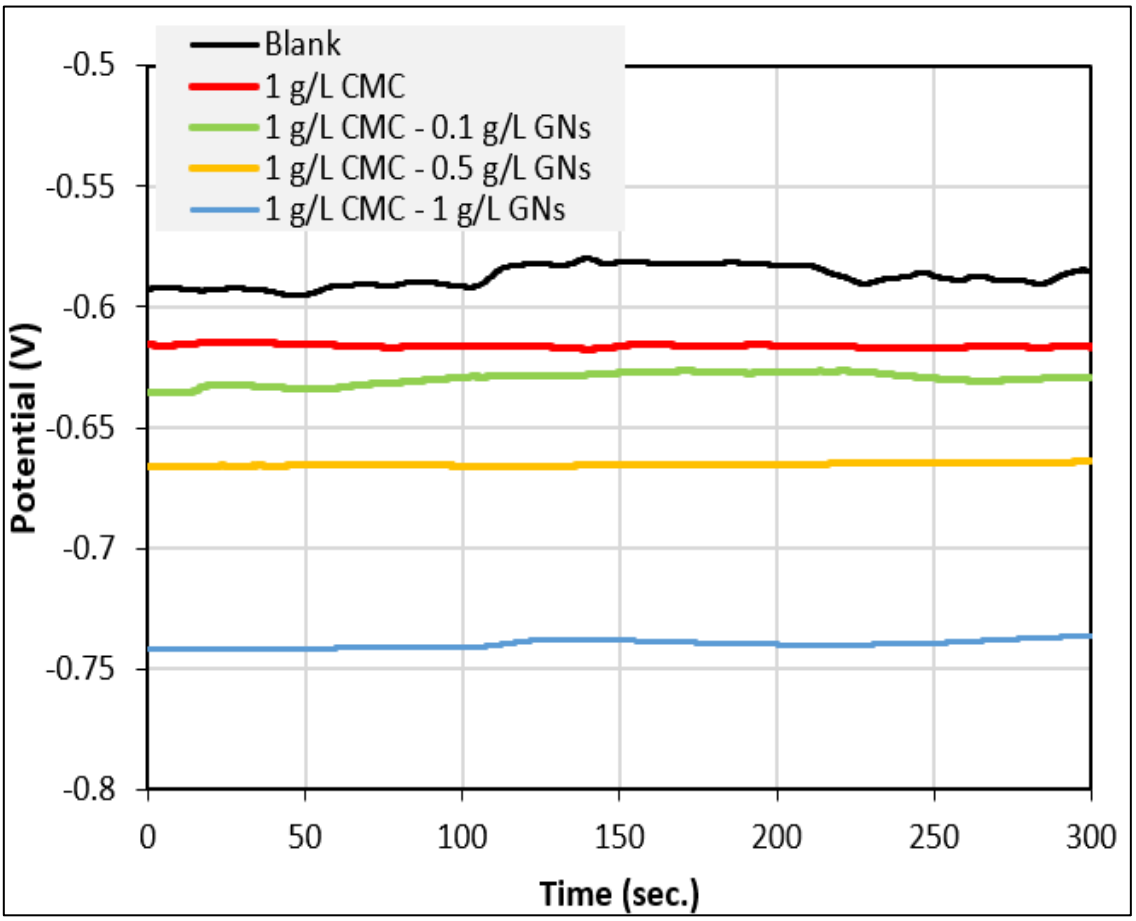

Figure 10. Potential-time relation in the absence and presence of CMC-GNs inhibitors at ambient temperature.

The potentiodynamic polarization behavior of low-carbon steel in saline media without and with CMC-GNs inhibitors is shown in **Figure 11**. **Figure 11a** presents the Tafel plots at 25°C, where the addition of CMC and CMC-GNs reduced the corrosion current density compared with the uninhibited saline solution. This result indicates that the inhibitor formed a protective layer on the steel surface at ambient temperature. Figure 11b shows the polarization curves at 35°C, where the inhibited systems still maintained lower corrosion activity, although temperature elevation began to affect the electrochemical response. **Figure 11c** presents the curves at 45°C, showing that CMC-GNs continued to suppress corrosion reactions under more aggressive thermal conditions. **Figure 11d** shows the polarization behavior at 55°C, where the inhibitor still provided protection, but the thermal effect increased the tendency of corrosion reactions. The polarization curves confirm that CMC-GNs acted as a mixed-type inhibitor by affecting both anodic metal dissolution and cathodic

reactions. This behavior is associated with the adsorption of CMC functional groups and the barrier effect of graphite nanosheets on the steel surface (Fares et al., 2010; Senthilvasan and Rangarajan, 2016).

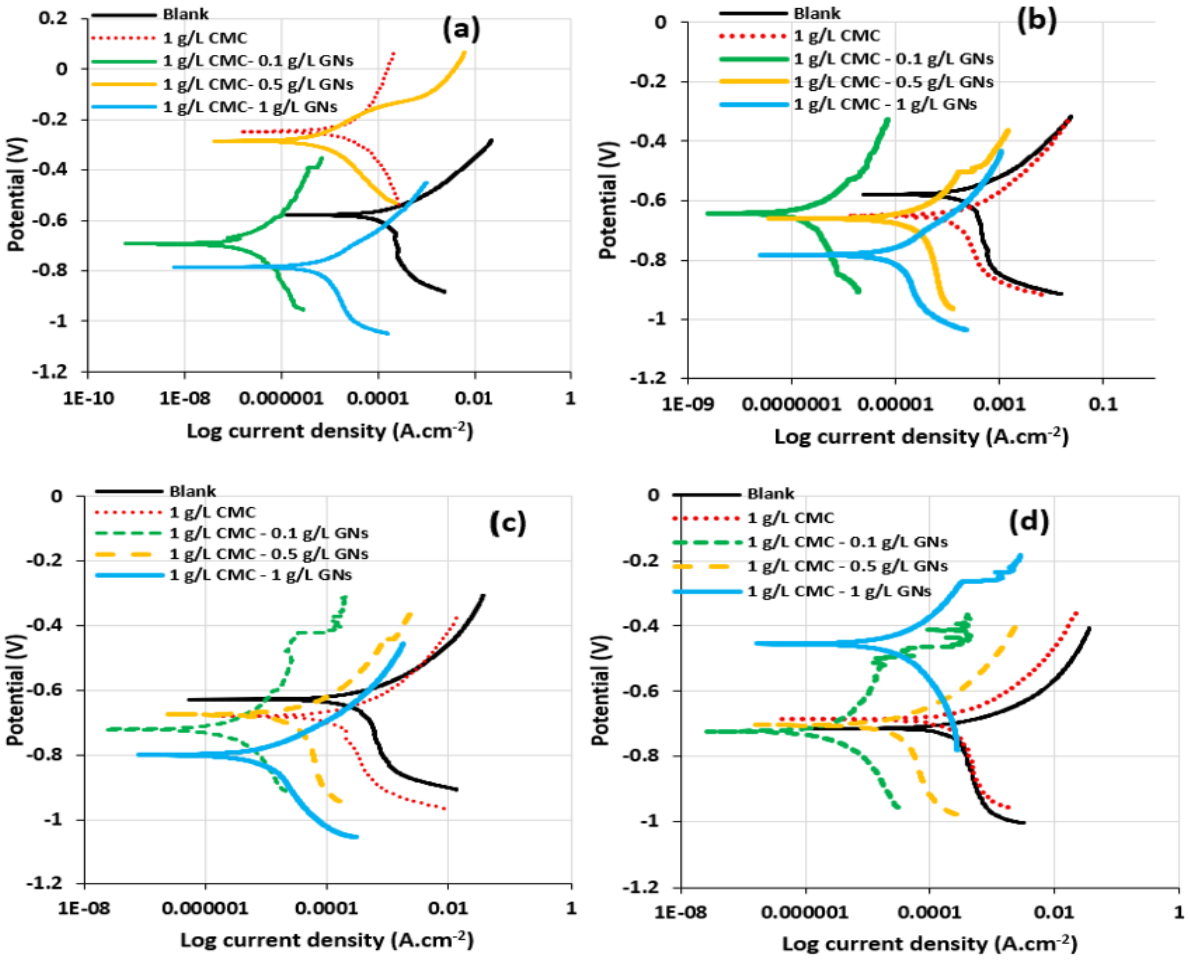

Figure 11. Tafel plots of low-carbon steel in saline media without and with CMC-GNs inhibitors at different temperatures: (a) 25°C, showing corrosion reduction at ambient temperature; (b) 35°C, showing continued inhibition under moderate thermal exposure; (c) 45°C, showing maintained protection under elevated temperature; and (d) 55°C, showing the inhibitor response under the highest tested temperature.

The polarization parameters obtained from the Tafel curves are summarized in **Table 1**. The addition of CMC and CMC-GNs reduced the corrosion current density of low-carbon steel compared with the uninhibited saline solution, confirming that the inhibitor suppressed electrochemical corrosion reactions. Among the tested formulations, CMC-GNs at 0.1 g/L provided the highest inhibition efficiency at all tested temperatures. This result indicates that a low nanosheet concentration produced more effective dispersion and more uniform surface coverage than higher concentrations. The improved inhibition performance can be attributed to the adsorption of CMC functional groups on the steel surface and the barrier effect of graphite nanosheets, which together limited chloride penetration and reduced active corrosion sites (Fares et al., 2010; Senthilvasan and Rangarajan, 2016).

Table 1. Polarization parameters of immersed low-carbon steel in various concentrations of dispersed CMC-GNs in saline solutions at different temperatures.

CONCENTRATION (g/L)	TEMPERATURE (°C)	$-E_{corr}$ (mV)	i_{corr}×10^{-3} (A.cm^{-2})	-b$_a$ (V.dec^{-1})	-b$_c$ (V.dec^{-1})	R_p×10^3 (Ω.cm^2)	IE (%)
Blank	25	0.582	0.215	0.1222	0.8386	0.2154	---
	35	0.579	0.307	0.0987	0.5825	0.1194	---
	45	0.628	0.523	0.1290	0.6205	0.0887	---
	55	0.714	0.665	0.1037	1.9871	0.0644	---
1 CMC	25	0.285	0.085	0.0399	0.0461	0.1093	60.465
	35	0.662	0.151	0.0847	0.0326	0.1203	50.814
	45	0.676	0.165	0.0907	0.0321	0.1213	68.451
	55	0.686	0.316	0.1034	0.0634	0.2009	52.481
1 CMC + 0.1 GNs	25	0.692	0.008	0.0770	0.0615	0.1748	96.279
	35	0.643	0.012	0.0467	0.0281	0.0896	96.091
	45	0.720	0.019	0.0282	0.0291	0.0732	96.367
	55	0.724	0.028	0.0406	0.0296	0.0875	95.789
1 CMC + 0.5 GNs	25	0.285	0.012	0.0778	0.0541	0.1632	94.418
	35	0.660	0.016	0.0497	0.0457	0.1217	94.788
	45	0.674	0.023	0.0236	0.0503	0.0821	95.602
	55	0.704	0.039	0.0198	0.0496	0.0723	94.135
1 CMC + 1 GNs	25	0.785	0.016	0.1372	0.3850	0.5168	92.558
	35	0.782	0.022	0.1424	0.3590	0.5209	92.833
	45	0.800	0.031	0.2036	0.2323	0.5543	94.072
	55	0.454	0.045	0.2640	0.3323	0.7517	93.233

The decrease in inhibition performance at higher CMC-GNs concentrations suggests that excessive nanosheet loading may promote partial aggregation, reduce the uniformity of the protective layer, and weaken the inhibitor distribution on the steel surface. Although higher graphite concentrations also improved corrosion resistance, their performance was lower than that of the lowest concentration. This behavior may be related to partial aggregation at higher nanosheet loading, which can reduce uniform coverage on the steel surface. Therefore, inhibition efficiency depends not only on the amount of nanomaterial but also on dispersion stability and surface-film uniformity. The best-performing formulation likely provided a balanced ratio between CMC adsorption and nanosheet distribution.

3.4. Electrochemical Impedance Spectroscopy

Electrochemical impedance spectroscopy was used to further evaluate the corrosion resistance of low-carbon steel in inhibited saline media. The Nyquist plots in **Figure 12** show larger semicircle diameters after adding CMC-GNs, indicating increased charge-transfer resistance. The fitted EIS parameters in **Table 2** show that the resistance values increased in the presence of CMC-GNs, confirming that the nanocomposite layer reduced charge transfer between the steel surface and electrolyte. This effect is associated with the adsorption of CMC functional groups and physical coverage by graphite nanosheets, which together create a compact barrier film.

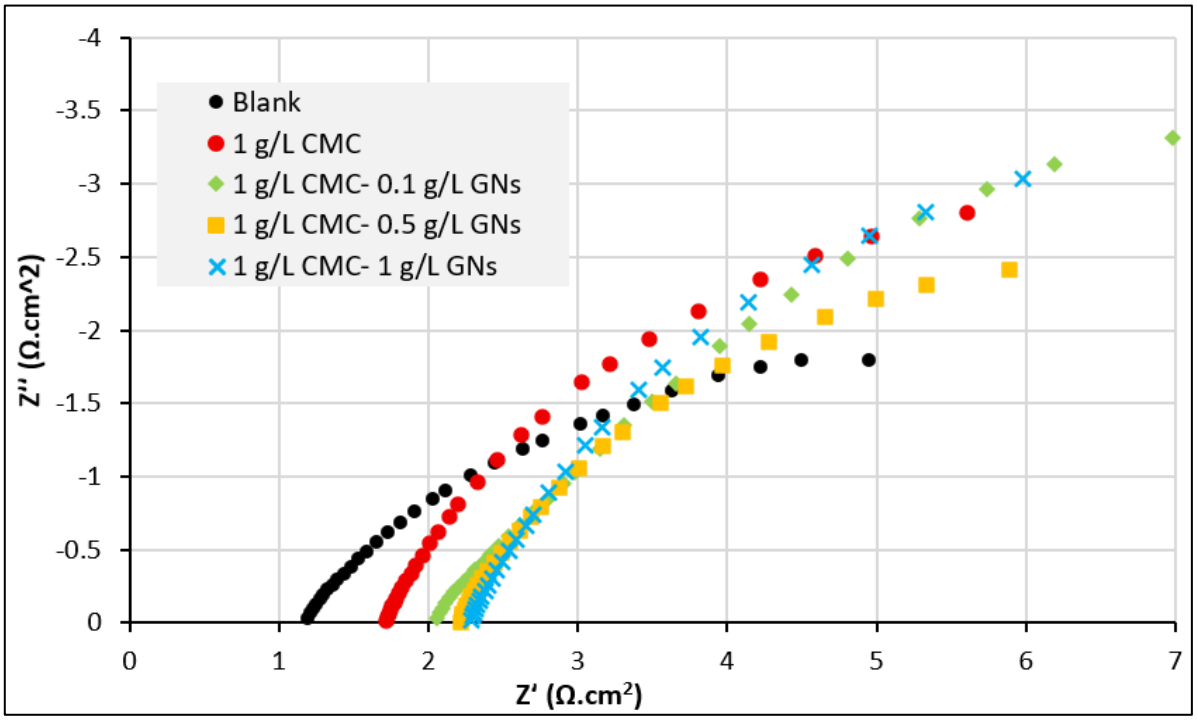

Figure 12. Nyquist plots of inhibition in the presence of CMC with different concentrations of GNs.

Table 2. EIS data of low-carbon steel treated in the presence of CMC-GNs inhibitor.

CONCENTRATION (g/L)	R_s ($\Omega.cm^2$)	R_{ct} ($\Omega.cm^2$)	C_{dl} (F)
0	1.410	2.496	0.567
1 CMC	1.744	3.849	1.378
1 CMC+ 0.1 GNs	2.001	5.223	1.644
1 CMC+ 0.5 GNs	2.245	6.382	1.652
1 CMC + 1.0 GNs	2.320	7.109	1.853

The long-term inhibition performance of the optimum CMC-GNs formulation was evaluated using Tafel polarization after different immersion periods, as shown in **Table 3** and **Figure 13**. **Figure 13a** shows the polarization curves at 25°C, where the CMC-GNs layer provided the strongest protection during early immersion and maintained inhibition during longer exposure. **Figure 13b** presents the curves at 35°C, indicating that the protective layer remained active, although corrosion current increased with longer immersion time. **Figure 13c** shows the response at 45°C, where higher temperature accelerated electrochemical activity and gradually weakened the protective film. **Figure 13d** presents the curves at 55°C, showing the most aggressive condition, in which thermal exposure and prolonged immersion reduced the resistance of the inhibitor layer. These results indicate that CMC-GNs can protect low-carbon steel during prolonged saline exposure, but the protection decreases when immersion time and temperature increase because ion mobility and chloride attack become stronger.

Table 3. Corrosion parameters of immersed low-carbon steel in CMC-GNs-based saline at various temperatures for a prolonged time.

IMMERSION TIME (DAYS)	TEMPERATURE (°C)	$-E_{cor}$ (mV)	$i_{corr}\times10^{-3}$ (A/cm^2)	$-b_a$ (mV/dec)	$-b_c$ (mV/dec)	R_p (Ω.cm^2)
1	25	0.248	0.0194	173.40	131.95	1677.10
	35	0.690	0.0213	167.50	155.08	1641.57
	45	0.701	0.0252	102.01	146.17	1035.24
	55	0.738	0.0315	107.41	103.07	725.04
3	25	0.765	0.2121	118.57	115.53	119.7970
	35	0.732	0.3014	108.17	118.34	81.4167
	45	0.742	0.4630	101.77	151.75	57.1296
	55	0.771	0.5876	121.69	153.26	50.1250
5	25	0.749	0.2449	139.14	67.19	80.3386
	35	0.738	0.3783	135.50	103.69	67.4222
	45	0.760	0.4842	135.61	110.61	54.6316
	55	0.780	0.5937	139.73	115.46	46.2377
7	25	0.792	0.2142	201.98	73.35	109.079
	35	0.762	0.3585	162.62	128.26	86.8497
	45	0.735	0.4630	102.55	169.10	59.8680
	55	0.753	0.5742	104.97	182.79	50.4232

3.5. Surface Morphology and Inhibition Mechanism

SEM analysis was used to compare the surface morphology of low-carbon steel before and after exposure to saline media, as shown in **Figure 14**. **Figure 14a** shows the freshly polished steel surface with a relatively smooth morphology and minor polishing marks. **Figure 14b** shows the steel surface after immersion in 3.5 wt.% NaCl solution without inhibitor, where severe surface damage, corrosion products, and cracks can be observed. This morphology confirms that chloride ions attacked the steel surface and promoted localized corrosion in the saline environment.

The inhibited surfaces show clear morphological improvement compared with the uninhibited sample. **Figure 14c** shows the steel surface protected with CMC, where a polymeric layer covered part of the surface and reduced visible corrosion damage. However, the coverage appears less uniform due to polymer clustering. **Figure 14d** shows the surface treated with CMC-GNs, where a smoother and more continuous protective layer was formed. The distributed bright areas can be associated with graphite nanosheets embedded in or attached to the CMC layer. This morphology indicates that CMC-GNs improved surface coverage and produced a more compact barrier against chloride penetration. Therefore, the corrosion protection mechanism is related to the combined adsorption of CMC functional groups and the physical shielding effect of graphite nanosheets.

EDX analysis was conducted to support the SEM observations and identify elemental changes on the steel surface after different treatments, as shown in **Figure 15**. **Figure 15a** presents the EDX spectrum of the polished low-carbon steel surface, where the signal is dominated by Fe as the main element of the substrate. **Figure 15b** shows the corroded steel surface after exposure to 3.5 wt.% NaCl solution, where oxygen and chloride-related

corrosion products indicate surface oxidation and chloride attack. **Figure 15c** shows the steel surface inhibited with CMC, where the increased carbon and oxygen signals indicate the presence of an adsorbed polymeric layer. **Figure 15d** shows the surface inhibited with CMC-GNs, where the carbon and oxygen signals are more evident, while the Fe signal decreases due to surface coverage by the polymeric nanocomposite. These elemental changes confirm that CMC-GNs formed a protective layer on the steel surface, limiting direct contact between the steel substrate and the saline electrolyte.

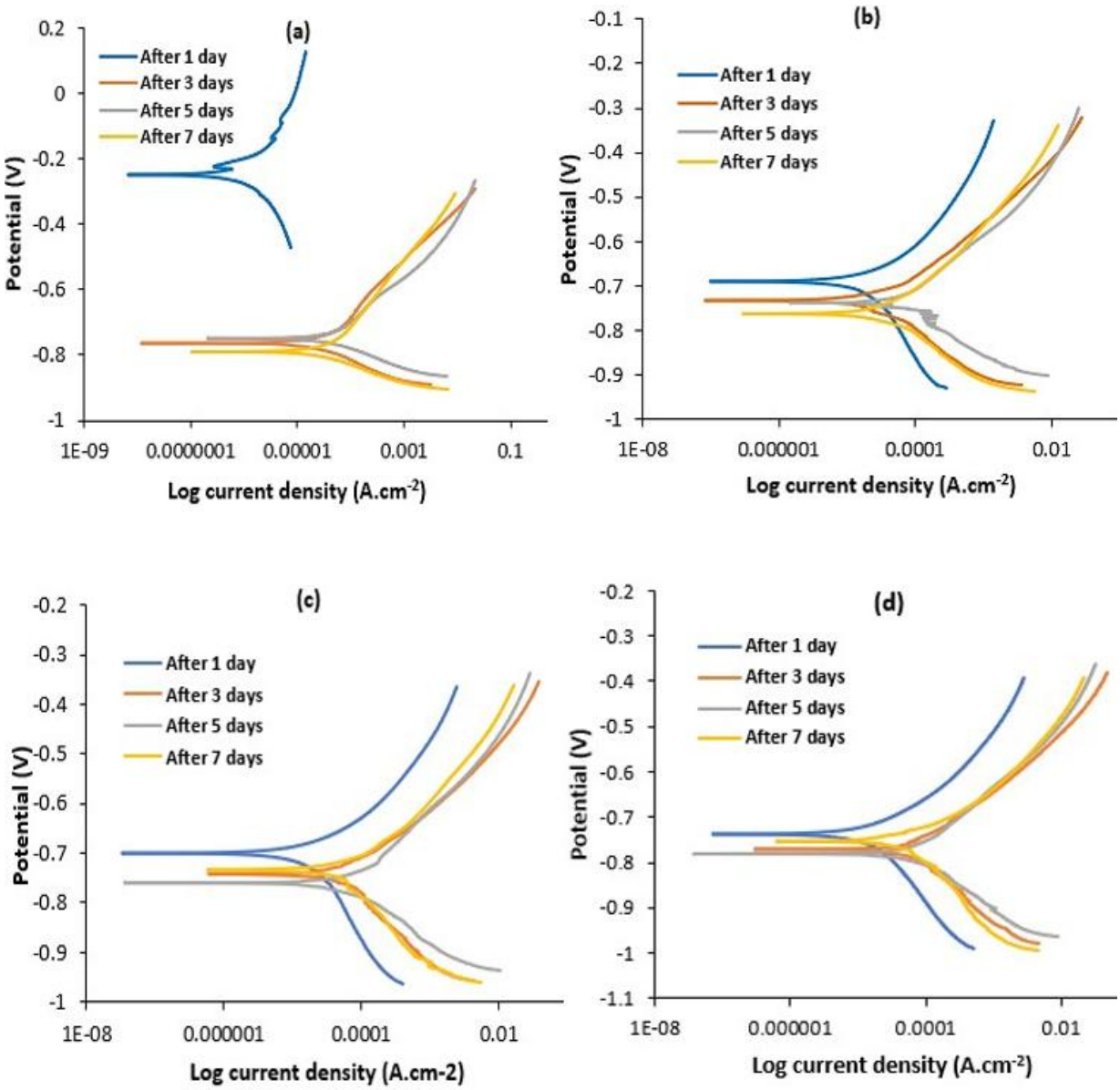

Figure 13. Tafel plots of low-carbon steel inhibited by the optimum CMC-GNs formulation at different immersion times and temperatures: (a) 25°C, showing the strongest long-term protection at ambient temperature; (b) 35°C, showing maintained but gradually reduced inhibition; (c) 45°C, showing increased corrosion activity under elevated temperature; and (d) 55°C, showing the inhibitor response under the most severe thermal condition.

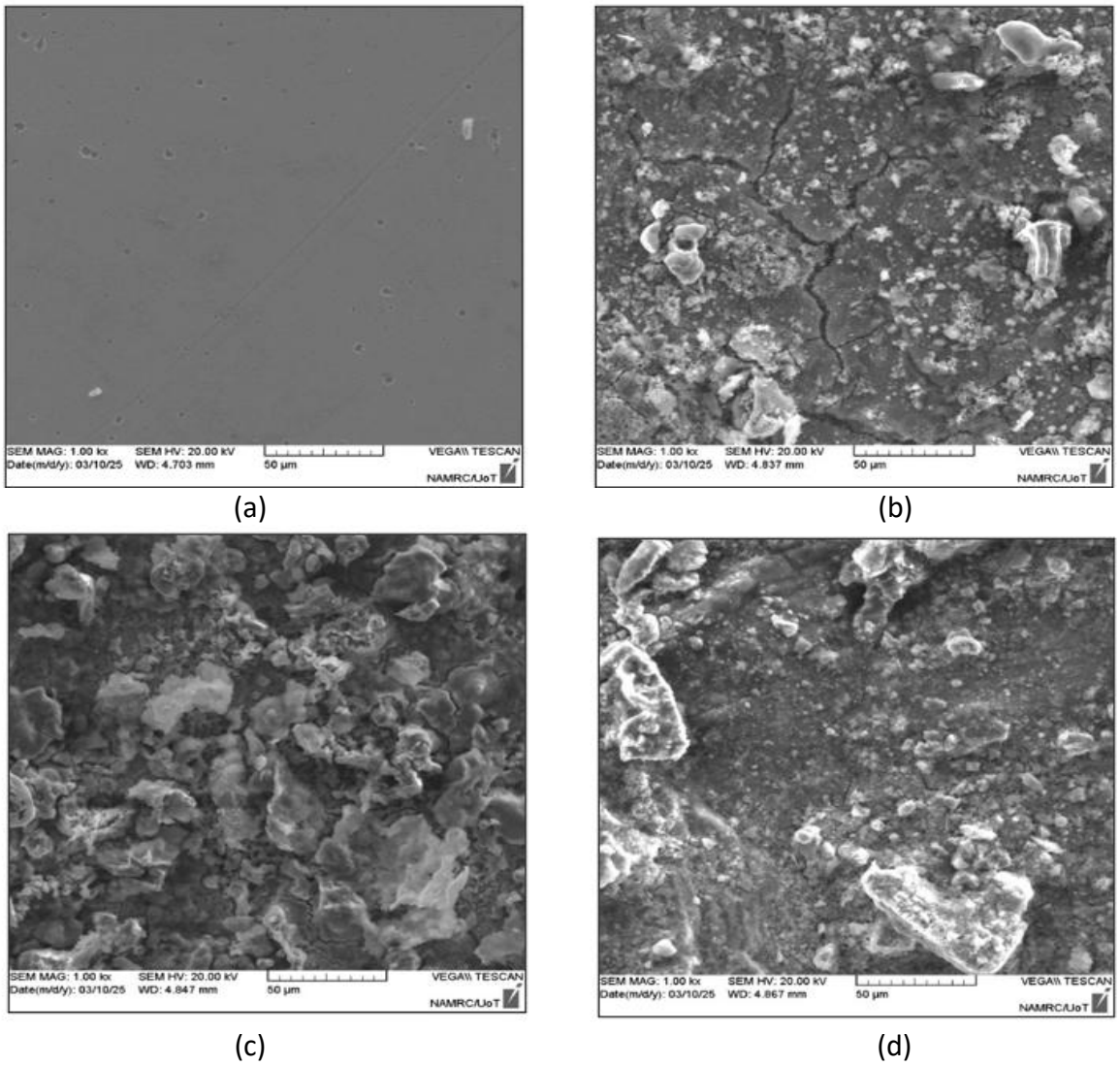

Figure 14. SEM images of low-carbon steel surfaces after different treatments: (a) freshly polished steel showing a relatively smooth surface with polishing marks; (b) steel corroded in 3.5 wt.% NaCl showing damaged surface, corrosion products, and cracks; (c) steel inhibited with CMC showing partial polymeric coverage and reduced damage; and (d) steel inhibited with CMC-GNs showing a smoother, more continuous, and more protective nanocomposite layer.

3.6. Bibliometric Analysis

The bibliometric trend of corrosion inhibitor research based on the Scopus search query TITLE-ABS-KEY (corrosion AND inhibitor) is presented in **Figure 16**. The search identified 43,119 documents published between 1928 and 2025. Corrosion inhibitor research remained relatively limited during the early decades, followed by gradual growth and then a sharp increase after the 2000s. The number of documents continued to rise in recent years. This increasing publication trend indicates that corrosion inhibitor research has become an active and expanding field. The rapid growth in recent years is consistent with the increasing demand for safer, more efficient, and environmentally responsible corrosion-control materials. In this context, the development of CMC-modified graphite nanosheets is relevant because the material combines a biodegradable polymer with a carbon-based nanosheet barrier to reduce corrosion activity in saline environments.

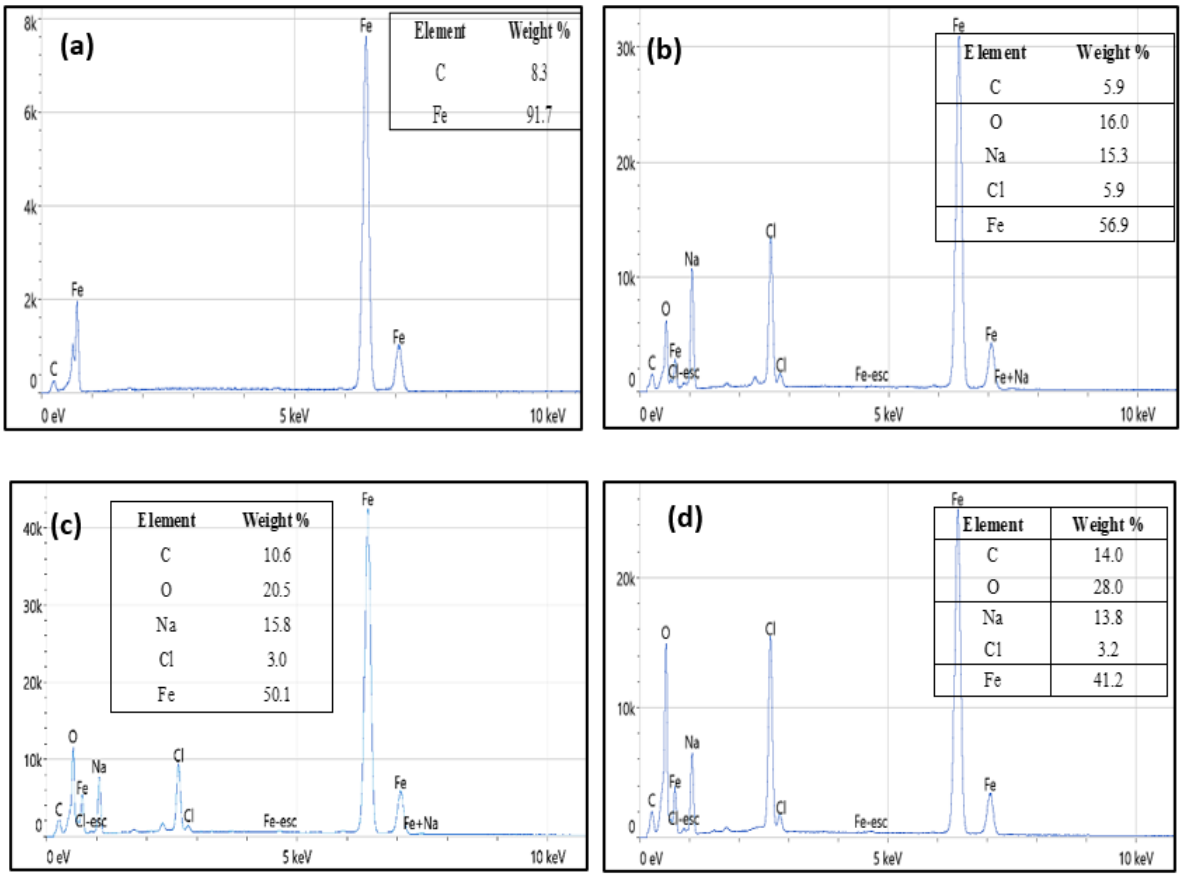

Figure 15. EDX spectra of low-carbon steel surfaces after different treatments: (a) polished steel dominated by Fe from the substrate; (b) steel corroded in 3.5 wt.% NaCl showing oxidation and chloride-related corrosion products; (c) steel inhibited with CMC showing carbon- and oxygen-containing polymeric coverage; and (d) steel inhibited with CMC-GNs showing stronger carbon and oxygen signals associated with nanocomposite protective-layer formation.

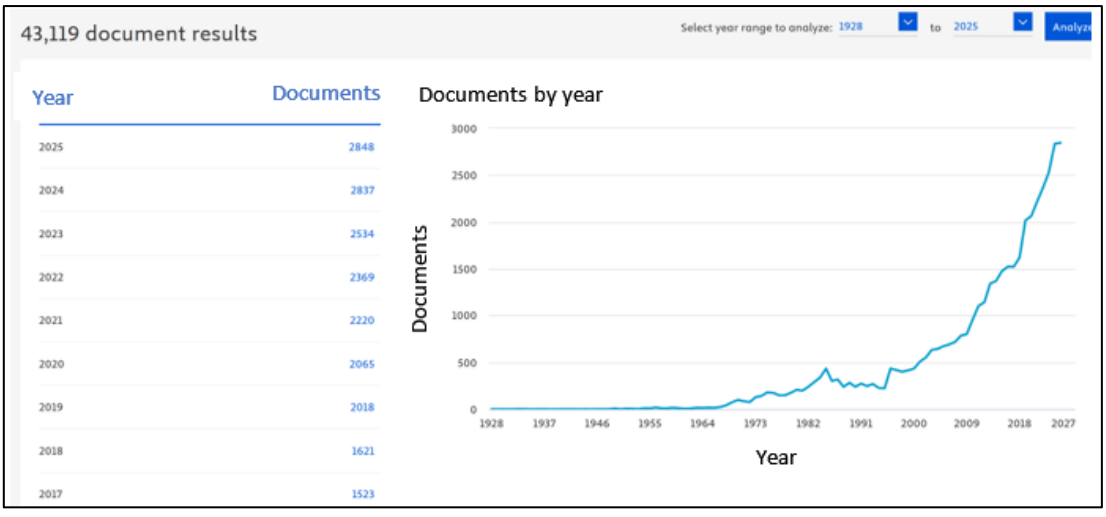

Figure 16. Bibliometric trend of corrosion inhibitor research based on the Scopus search query TITLE-ABS-KEY (corrosion AND inhibitor) from 1928 to 2025. The figure shows 43,119 document results and an increasing number of annual publications, especially after the 2000s, indicating the growing research attention to corrosion inhibitor development. Data was taken in June 2026.

3.7. Relevance of CMC-GNs Corrosion Inhibitor to SDGs

The development of CMC-GNs as an eco-friendly corrosion inhibitor is relevant to SDGs-oriented materials engineering because it combines corrosion protection, biodegradable polymer chemistry, and reduced dependence on hazardous inhibitor systems. Low-carbon steel is widely used in industrial, marine, and oilfield infrastructure; therefore, improving its durability in saline environments can reduce material failure, maintenance frequency, and replacement demand. CMC-GNs formed a protective layer on the steel surface, reduced corrosion activity, and maintained inhibition performance under saline and thermal exposure. These findings indicate that the proposed inhibitor supports more sustainable infrastructure protection by extending steel service life and reducing corrosion-related resource consumption (Verma et al., 2021).

The relevance of the SDGs to this study is summarized in **Table 4**. The strongest contribution is related to SDG 9 because corrosion protection directly supports infrastructure durability and industrial reliability. The use of CMC as a biodegradable and water-soluble polymer also supports SDG 12 because it promotes responsible material selection and may reduce dependence on toxic conventional inhibitors. In addition, protection of steel in saline and marine-related environments supports SDG 14 by helping reduce chemical risks and metal deterioration in chloride-rich systems. The combination of material performance and bibliometric evidence shows that green corrosion inhibitors are part of a growing research direction toward sustainable engineering solutions.

Table 4. Relevance of CMC-GNs corrosion inhibitor development to selected SDGs.

SDG	RELEVANCE TO THIS STUDY	CONTRIBUTION OF CMC-GNS INHIBITOR
SDG 9: Industry, innovation, and infrastructure	Low-carbon steel is used in pipelines, storage tanks, oilfield equipment, and saline-service infrastructure.	Enhances corrosion protection and supports the longer service life of steel components in aggressive environments.
SDG 12: Responsible consumption and production	Conventional corrosion inhibitors may involve toxicity, instability, or environmental concerns.	Uses CMC as a biodegradable polymer and supports the development of safer, eco-friendly inhibitor systems.
SDG 14: Life below water	Saline and marine-related environments accelerate steel corrosion and may increase chemical and material contamination risks.	Provides a protective strategy for steel exposed to chloride-rich media while supporting reduced reliance on hazardous inhibitors.
SDG 13: Climate action	Frequent replacement of corroded steel components can increase material and energy consumption.	Supports durability improvement, which may indirectly reduce resource use associated with repair, replacement, and maintenance.

The CMC-GNs inhibitor provides a practical contribution to SDGs-oriented corrosion protection by combining material efficiency with environmental considerations. The use of a polymeric nanocomposite barrier can reduce corrosion activity in saline environments, while the selection of CMC supports greener material design. Therefore, this study contributes not only to corrosion science but also to sustainable materials development for industrial and marine infrastructure.

4. CONCLUSION

CMC-modified graphite nanosheets were successfully prepared as an eco-friendly inhibitor for low-carbon steel in saline environments. The nanocomposite showed stable dispersion, effective adsorption, and strong corrosion inhibition because CMC functional groups promoted surface attachment while graphite nanosheets improved barrier protection against chloride penetration. Electrochemical results confirmed lower corrosion activity, and SEM-EDX observations verified protective-layer formation on the steel surface. The optimum formulation maintained protection under saline and thermal exposure, although prolonged immersion reduced resistance. These findings indicate that CMC-GNs can support SDGs-oriented corrosion control by reducing reliance on toxic inhibitors and improving the durability of steel infrastructure in marine and industrial systems.

5. ACKNOWLEDGMENTS

We express gratitude to the University of Technology, Baghdad, Iraq, and the Nanotechnology and Advanced Materials Research Center for supporting the experimental part of this research work.

6. AUTHORS' NOTE

The authors declare that there is no conflict of interest regarding the publication of this article. The authors confirmed that the paper was free of plagiarism.

7. REFERENCES

Akhlaq, M., Mushtaq, U., Naz, S., and Uroos, M. (2023). Carboxymethyl cellulose-based materials as an alternative source for sustainable electrochemical devices: A review. *RSC Advances, 13*(9), 5723-5743.

Anaee, R. A. M. (2014). Thermodynamic and kinetic study for corrosion of Al-Si-Cu/Y_2O_3 composites. *Asian Journal of Chemistry, 26*(14), 4469-4474.

Borode, A. O., Ahmed, N. A., and Olubambi, P. A. (2021). Electrochemical corrosion behavior of copper in graphene-based thermal fluid with different surfactants. *Heliyon, 7*(1), e05949.

Fares, M. M., Maayta, A. K., and Al-shawabkeh, A. F. (2010). Carboxymethyl cellulose as corrosion inhibitor of iron in the presence of magnetic field; kinetic investigation. *Journal of Corrosion Science and Engineering, 13*(27), 1-15.

Fathima, A. A., Geethanjali, R., and Subhashini, S. (2015). Polymeric corrosion inhibitors for iron and its alloys: A review. *Chemical Engineering Communications, 202*(2), 232-244.

Ghanem, A. F., and Abdel Rehim, M. H. (2018). Assisted tip sonication approach for graphene synthesis in aqueous dispersion. *Biomedicines, 6*(2), 63.

Kumar, B., and Priyadarshi, R. (2020). Nanoporous sodium carboxymethyl cellulose-g-poly(sodium acrylate)/$FeCl_3$ hydrogel beads: Synthesis and characterization. *Gels, 6*(4), 49.

Najm, N., Ataiwi, A. H., and Anaee, R. A. (2022a). Effect of indium coating on corrosion behavior of AZ31 Mg alloy by DC sputtering. *Materials Today: Proceedings, 62*, 4551-4555.

Najm, N., Ataiwi, A. H., and Anaee, R. A. (2022b). Annealing and coating influence on the mechanical properties, microstructure, and corrosion properties of biodegradable Mg alloy (AZ91). *Journal of Bio- and Tribo-Corrosion, 8*(2), 64.

Ren, H., Gao, Z., Wu, D., Jiang, J., Sun, Y., and Luo, C. (2016). Efficient Pb(II) removal using sodium alginate-carboxymethyl cellulose gel beads: Preparation, characterization, and adsorption mechanism. *Carbohydrate Polymers, 137*, 402-409.

Salama, A., Shukry, N., and El-Sakhawy, M. (2015). Carboxymethyl cellulose-g-poly(2-(dimethylamino)ethyl methacrylate) hydrogel as adsorbent for dye removal. *International Journal of Biological Macromolecules, 73*, 72-75.

Senthilvasan, P. A., and Rangarajan, M. (2016). Corrosion inhibition properties of graphene oxide on mild steel in 3.5% NaCl. *IOP Conference Series: Materials Science and Engineering, 149*, 012064.

Shao, H., Li, D., Chen, Z., Yin, X., Chen, Y., Liu, Y., and Yang, W. (2024). Sulfur dots corrosion inhibitors with superior antibacterial and fluorescent properties. *Journal of Colloid and Interface Science, 654*, 878-894.

Sharma, V., Garg, A., and Sood, S. C. (2015). Graphene synthesis via exfoliation of graphite by ultrasonication. *International Journal of Engineering Trends and Technology, 26*(1).

Solomon, M. M., Umoren, S. A., Udosoro, I. I., and Udoh, A. P. (2010). Inhibitive and adsorption behaviour of carboxymethyl cellulose on mild steel corrosion in sulphuric acid solution. *Corrosion Science, 52*(4), 1317-1325.

Tiu, B. D. B., and Advincula, R. C. (2015). Polymeric corrosion inhibitors for the oil and gas industry: Design principles and mechanism. *Reactive and Functional Polymers, 95*, 25-45.

Umoren, S. A., and Eduok, U. M. (2016). Application of carbohydrate polymers as corrosion inhibitors for metal substrates in different media: A review. *Carbohydrate Polymers, 140*, 314-341.

Verma, C., Ebenso, E. E., Quraishi, M. A., and Hussain, C. M. (2021). Recent developments in sustainable corrosion inhibitors: Design, performance and industrial scale applications. *Materials Advances*, *2*(12), 3806-3850.

Verma, C., Verma, D. K., Ebenso, E. E., and Quraishi, M. A. (2018). Sulfur and phosphorus heteroatom-containing compounds as corrosion inhibitors: An overview. *Heteroatom Chemistry, 29*(4), e21437.

Xu, H., and Suslick, K. S. (2011). Sonochemical preparation of functionalized graphenes. *Journal of the American Chemical Society, 133*(24), 9148-9151.

Yu, W., and Xie, H. (2012). A review on nanofluids: Preparation, stability mechanisms, and applications. *Journal of Nanomaterials, 2012*(1), 435873.